

A Dynamic Subgoal Path Planner for Unpredictable Environments

Hong Liu, Weiwei Wan and Hongbin Zha

Abstract—Although lots of planning algorithms have focused on the planning of fixed manipulators and mobile robots in moderate dynamic environments, seldom planning algorithms can be employed to deal with mobile agents in the presence of large scenario scales and unpredictable changing obstacles. Path planning for mobile robots in unpredictable environments would be an extreme challenge since computational complexity increase dramatically with high dimensionality, unpredictability and large scales. In this paper, a novel and real-time approach is proposed to solve this problem by generating subgoals dynamically according to time and potential values. This dynamic subgoal based approach includes two procedures, the subgoal generator and the inter-subgoal or inner replanner. On the one hand, a set of high-level subgoals is generated dynamically by an improved single shot strategy that could tailor itself adaptively. On the other hand, a roadmap is built during the preprocessing phase by employing a localized Dynamic Roadmap Mapping (local-DRM) for inter-subgoal replanning. Finally these two procedures will collaborate according to the potential field criterion to ensure completeness. Our approach can not only generate paths rapidly enough to satisfy the requirements of an anytime planner but also work for large scenario scales. Experimental results on different kinds of mobile agents, in large scenario scales and in the presence of unpredictable changing obstacles show that our approach can find out a collision free path on an average of 0.11s for a single planning, indicating an anytime planner.

I. INTRODUCTION

Since the presence of random algorithms, such as the popular probabilistic roadmap method (PRM)[1] and the rapidly-exploring randomized tree method (RRT)[2] method, path planning study has improved significantly. The derivatives of these algorithms can not only solve the traditional piano mover's problems, but also be competent for path planning in moderate dynamic environments[3][4]. However, this is not always the case in unpredictable environments. Recent progresses[5][6] seek to solve such problems by the idea of anytime planning. Their works are promising because their realtime performance. However, such a problem remains challenging due to high DOFs, large scenario scales and unpredictable changing obstacles.

In this paper, we seek an anytime solution based on the idea of dynamic subgoals where single query and multiple query primitives are borrowed as subgoal generator and inter-subgoal replanner respectively. Single query strategy[7] will

find a collision free path for robots without the preprocessing phase. Generally speaking, it is much faster than a multiple query strategy taking into account the consumptive preprocessing phase of the later one. Like heuristic searching algorithms, single query strategy tries to consider as less redundant configurations as possible to generate feasible paths. This is usually realized by a goal-biased sampling scheme since there is no need for a complete planner in most scenarios. References [2] and [8] are examples of this strategy. Although single query strategy plays an important role in changing environments where multiple query strategy (PRM and its variants[9][10]) seems infeasible, it is not efficient enough for anytime requisites. On the contrary, multiple query strategy can take advantage of the prebuilt roadmaps to rapidly replan motions. DRM [11][12][13], which is a derivative of PRM, can effectively plan for fixed base manipulators or high-DOF robots by employing a mapping between W space and C space. It can find a collision-free path in the presence of both stationary and changing obstacles and can satisfy the requisites of an anytime planner. Nevertheless, the planner encounters great challenges when these manipulators or robots are mounted on mobile bases. (1) The increased C Space dimensions require more samples or a more sophisticated sampling schema. (2) The movements of obstacles become more drastic due to relative motion. (3) The extension of W Space makes $W-C$ mapping more complicated.

The collaboration of these primitives helps a lot in overcoming those shortages. For one thing, subgoals from single query primitives can help reduce the size of W space and the amount of configurations required for mapping. For another, multiple query primitives can replan rapidly in a inter-subgoal space and improve the efficiency of tree exploring. At first, the single query based procedure explores in relatively large steps with a adaptively increasing biased probability and generates pivots that are called subgoals without checking configurations along the edges between them. Then, these subgoals will be treated as query configurations and submitted to the multiple query based procedure for inner replanning. From another viewpoint, this is like the lazy evaluation strategy[10] where lazy collision detection is innovated by local planning. This idea is from what people do in their daily motion planning. People would not or cannot plan specific motions far away when one is in a new environment. Usually, what they are going to do is moving toward their destination or destination lists with only local planning. Here the subgoals play the role of destination lists. The global director is the single query procedure that moves a man toward the goal direction, while the inter-subgoal

Hong Liu is with the Key Lab of Machine Perception and Intelligence and the Key Lab of Integrated Micro-System, Shenzhen Graduate School, Peking University, China. hongliu@pku.edu.cn

Weiwei Wan is with the Key Lab of Machine Perception and Intelligence, Peking University, China wanweiwei@cis.pku.edu.cn

Hongbin Zha is with the Key Lab of Machine Perception and Intelligence, Peking University, China zha@cis.pku.edu.cn

planner is the multiple procedure. Note that the subgoals in our approach are always changing according to time and potential values (refer to Section V), we name them dynamic subgoals.

Our main contributions are planning in unpredictable environments as following.

- Mobile robots usually encounters relatively large scales due to their mobility. The planner in this paper can dynamically generate paths in large scenarios.
- Changes of obstacles become unpredictable due to their movements and relative motions. The planner can avoid the obstacles and reach the destination tactically.

The rest of this paper is organized as follows. Related works are presented in Section II. Section III discusses anytime planning. In Section IV and Section V, details and the overall framework of the planner are presented respectively. Experiments and analysis are introduced in Section VI. Section VII draws the final conclusions followed by acknowledgement.

II. BACKGROUND WORKS

The idea of subgoals is not new and relates to many previous works and the concept of subgoals has been employed to reduce computational complexity of planning paths for long[15][16]. However, subgoals in these articles cannot be transplanted into our scenario directly due to the requirement of efficiency for an anytime planner. Typical approaches usually store those pregenerated subgoals for future usage. Yet such storage helps little in changing environments. For instance, suppose that there is a sequence of subgoals G_i in the subgoal list L_{sg} . Then there will be a time period T_i for each subgoal position G_i that a robot cannot arrive at in T_i . Due to the motions of obstacles, G_i may become obstructed after such a T_i (or when the robot arrives at G_i). Consequently, it is helpless to store G_i and replanning should be performed in T_i to generate new subgoals for replanning. In this case, the subgoal problem in this paper becomes different from those related works and we must attempt new solutions. These subgoals are not employed to store information but act as pivots to the final aim. Since the environments change along time, these subgoals are regenerated according to the change, namely dynamic subgoals.

Another idea is the collaboration of single query and multiple query primitives. Sampling based Roadmap of Trees(SRT)[14] is a pioneer of this idea. In SRT, configurations in the preprocessed roadmap are substituted by single query trees. SRT can better model C_{free} spaces and does well in complicated environments (narrow spaces). However, SRT is not suitable for realtime applications although it can refer to parallelized computing to improve its efficiency. Unlike SRT, the approach in this paper is fast enough on ordinary processors and seeks a balance between completeness and efficiency.

III. ANYTIME PLANNING

The key point of a planner for unpredictable changing environments is rapid replanning at any necessary time. And the key point of an anytime planner is to plan online with as less time as possible. In this section requisites of such a planner will be discussed. In reality, when obstacles are perceived at a specified time t_w , planners could usually start the computation immediately. However, motions cannot be carried out until $t_w + \tau$ where τ is the period of time required for planning the path. In a scenario s , τ must satisfy the inequation $\tau < t_s$ where t_s implies the dynamic attribute of the current scenario1, namely how the obstacles are changing. τ and t_s are illustrated in detail as following.

- τ The smaller τ is, the faster the planner will be.
- t_s A smaller t_s denotes an environment with more drastically moving obstacles.

In summary, an anytime planner should be able to generate a path as quickly as possible to lower τ and to satisfy a small enough t_s on the premise of a given completeness. See Fig.1 to fix the idea.

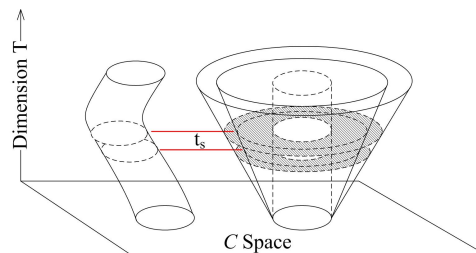


Fig. 1. An illustration of CT space obstacles and the idea of t_s .

When trajectories of obstacles are known or predictable, CT obstacles is like an extracted C space obstacle along the time dimension. The left object in Fig.1 demonstrates such an obstacle. When the environment is unpredictable, CT obstacles cannot be represented in a particular shape anymore. We could only roughly say that the obstacles in such case are contained in a truncated cone (see the right object of Fig.1). Here the slope of the frustum surface is subject to the differential constraints of the environment. In reality, the higher the surface slope is, the smaller the t_s should be. See the distance along the time dimension between the two red lines (the distance indicates t_s here) in Fig.1 to fix the idea. It lies in the fact that regarding a scenario with drastically moving unpredictable objects, the textured volume of the truncated cone becomes much larger and only a small enough t_s can guarantee safe motions. Another way to explicate t_s is a smaller t_s promises more drastic changes of an unpredictable obstacle.

In our approach, the subgoal generator and inner replanner are mainly from RRT and DRM. Raw RRT structures are developed to quickly explore C space. They can rapidly select larger Voronoi regions for expansion. The complexity of RRT depends on the length of the solution path while the length of the solution path depends on the selection of parameters δ_q and P_b . Here, δ_q is the step mounted to q_{near}

on the direction to q_{rand} and P_b is the probability of a new random sample being the goal configuration (refer to reference[2]). Formula (1) shows the role of δ_q .

$$q_{new} = q_{near} + \delta_q \quad (1)$$

Here, q_{new} will be added to the tree if it is collision free. Despite the fact that larger δ_q and P_b would lower the complexity of RRT significantly, they should not be tuned arbitrarily. Firstly, if a step δ_q is too large, some obstacles that obstruct the edge between q_{near} and q_{rand} in the C space may be overlooked and the path may become invalid. Secondly, P_b should not be too high either. Although higher P_b s give strong heuristics to goal points, they should be carefully chosen. In the worst case of $P_b = 1$, the RRT algorithm degenerates into a segment connector between the initial configuration and the goal one. Indeed, a higher P_b may lead RRT to local minima with a higher probability and hinder its application in generalized scenarios. In this paper, δ_q is enlarged to guarantee an efficient RRT while P_b is tuned adaptively to avoid local minima and ensure a smooth result.

DRM is different from the other multiple query strategies. It can replan at any time in the presence of unpredictable changing obstacles[11][12]. The algorithm is realized by constructing two kinds of mapping, a node mapping and an edge mapping.

$$\Phi_v(\omega) = \{v_i \in V | \Omega(v_i) \cap \omega \neq \emptyset\} \quad (2)$$

$$\Phi_e(\omega) = \{e_i \in E | \Omega(e_{ij}) \cap \omega \neq \emptyset, e_{ij} \in e_i\} \quad (3)$$

Here, $G = (V, E)$ is the roadmap constructed in C space during the preprocessing phase. V denotes the vertex set of the roadmap and the edge set is represented by symbol E . v_i and e_i indicate elements of V and E respectively. Suppose that an edge e_i can be subdivided into k succeeding configurations according to the requirement of a real application, symbol e_{ij} denotes the j th subdivided configuration along the edge e_i . DRM algorithms consider W space to be composed by voxels. That is, it divides W space into an array of cubes. ω in the equation denotes the voxels or cubes in W space. $\Phi_v(\omega)$ indicates the set of vertex configurations whose representative voxels include ω , or the set of vertex configurations that occupies ω . Like $\Phi_v(\omega)$, $\Phi_e(\omega)$ denotes the set of configurations on edges whose representative voxels include ω , or the set of edge configurations that occupies ω . Here, $\Phi_v(\omega)$ and $\Phi_e(\omega)$ are called vertex mapping and edge mapping respectively. The mapping $\Omega(p)$ indicates all the representative voxels of a configuration p . Through these definitions the vertices and edges that become invalid when ω is obstructed by obstacles can be easily found. As illustrated previously, DRM encounters fatal drawbacks on mobile robots. Fig.2 demonstrates the difference of DRM applying to a mobile humanoid robot.

When a manipulator is fixed on a base, the size of W space is fixed. In this case, the accessible W space of the manipulator can be divided into a limited number of ω . And $\Phi_v(\omega)$ and $\Phi_e(\omega)$ can be easily generated in

the preprocessing phase for the later invalidation. However, when robots become mobile (see Fig.2), simple mapping is no longer feasible. Firstly, there are at least three more DOFs due to the mobility of the robot. This implies that more DOFs should be sampled in the preprocessing phase. Then, the accessible W space may become so large that the exponentially increasing ω number quickly results in a too large mapping. It could be still possible to map W space in the left scenario of Fig.2. But in the right larger scenario it is completely infeasible. However, the primitives behind it are worthwhile and employed in our local procedure.

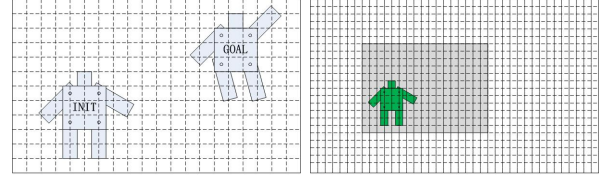


Fig. 2. DRM mapping applied to a mobile humanoid robot.

In this paper, we try to combine single query and multiple query primitives to make up respective drawbacks and improve performance. In order to improve the efficiency of RRT, we can tune δ_q and P_b . In order to apply DRM to mobile robots, we can lay limitations on the accessible range of W space. In our work, RRT primitives play the role of a high level guide as subgoal generators while DRM primitives will perform a detailed planning between those subgoals. Thanks to the attendance of DRM primitives, RRT could be enlarged since it no longer needs to care about those overlooked obstacles. DRM will plan locally and make a detour from the obstructed path. Thanks to the attendance of RRT primitives, DRM no longer needs to take into account areas δ_q step away. In this way the W space becomes limited and mappings inside the RRT step area can be competent for local planning.

IV. SUBGOAL GENERATOR AND INNER REPLANNER

Primitives from RRT and DRM play the role of the two procedures employed in our approach, namely the subgoal generator and the inner replanner respectively. Details of them will be shown in the following subsections.

A. Subgoal Generator

The subgoal generator is a modified RRT based on the raw structure. RRT has many derivatives, for example RRT-connect[17] or those stores previous experiences[18][19][20]. Nevertheless, employing a more complicated variation here is unnecessary. As configurations G_i at a long distance away is not going to be arrived before time T_i , samples at these G_i might become invalid due to the unpredictable movements of obstacles. Therefore, it is a waste of time to employ those variations that utilizes 'far away' information and only the elementary primitives are considered.

The modified RRT generator in this work is as following. Each time when replanning is invoked, the generator

regenerates a path with a large δ_q and an adaptively tuned P_b dynamically. See Algorithm 1 for details. The tuning of P_b is highly dependent on the core of collaboration (namely when to replan), and it will be explicated in Section V.

Algorithm 1: Subgoal Generator

Input: C_{init}^{global}
Output: $L^{globalpath}$

```

1  $G_{global}.init(C_{init}^{global});$ 
2 while True do
3    $C_{rand} \leftarrow biased\_rand\_conf(P_b);$ 
4    $C_{near} \leftarrow nearest\_vert(C_{rand}, G_{global});$ 
5    $C_{new} \leftarrow new\_conf(C_{near}, \delta_q);$ 
6   if not  $check\_collision(C_{new})$  then
7      $G_{global}.add\_vertex(q_{new});$ 
8     if  $check\_dist(C_{new}, C_{goal}^{global}) \leq \delta_q$  then
9        $L^{globalpath} \leftarrow back\_trace(C_{goal}^{global}, G_{global});$ 
10      return  $L^{globalpath};$ 
11    end
12  end
13 end

```

The input of the algorithm is C_{init}^{global} which denotes the configuration when replanning is required. The output $L^{globalpath}$ is a list of configurations indicating the path generated by this global search strategy. G_{global} denotes the exploring tree built during the generating of $L^{globalpath}$. C_{rand} , C_{near} and C_{new} are the same as those variables defined in a raw RRT planner, meaning different configurations employed when building the searching tree. A C_{rand} is acquired by a biased random sampling strategy with the probability P_b , that is the function $biased_rand_conf()$. The nearest vertex to C_{rand} in tree G_{global} is chosen as C_{near} in function $nearest_vert()$. Function $new_conf()$ moves C_{near} along the edge between C_{near} and C_{rand} with a step δ_q to generate C_{new} .

When replanning is required, the planner will first regenerate a global path $L^{globalpath}$ with input of the current configuration, namely C_{init}^{global} in Algorithm 1. Step δ_q in this subgoal generator is relatively large to improve the efficiency of raw RRT. Lines 8-10 show the criterion for termination. A new $L^{globalpath}$ is returned by back tracing the exploring tree when C_{new} is in the vicinity of C_{goal}^{global} . The back tracing procedure is implemented by function $back_trace()$.

B. Inner Replanner

The inner replanner is a localized DRM. Although the primitives (the mapping strategies, A* search) of DRM are employed in our local procedure, the local DRM focuses on different aspects.

- How to scale DRM to mobile robots working in arbitrary large scenarios
- How to make up the incompleteness of DRM mapping

This subsection will concentrate on the first aspect and the second aspect will be discussed in Section V.

1) *Localizing:* A local DRM tries to plan a local path for mobile robots locally. It only plans paths in a local C space without considering the whole W space which is neither possible to be known in advance nor solved or mapped in polynomial time. In this paper, DRM W space is localized to solve this problem. See the shadow region in the right of Fig.2 to fix the idea of a localized W space.

When a global path is generated by the subgoal generator, local DRM will employ these subgoals to plan locally. Local DRM will first update the invalidation of its V and E in the prebuilt local roadmap G_{DRM} . Then the two configurations will be inserted into G_{DRM} for A* search. Note that the insertion of query configurations is carried out after updating G_{DRM} and this indicates that the edges between query configurations and G_{DRM} are supposed to be collision-free. Lazy evaluation between the query configurations and G_{DRM} will be performed online when execution starts. Although this is a relatively time consuming procedure, it does little harm to our 'anytime' timer since only two edges at most are detected finally in one local search.

Besides, note that there is a high probability a path may not be found by the succeeding A* algorithm on the localized roadmap. This is highly relevant to the replanning schema and will be discussed in Section V.

2) *Implementation of mapping:* Instead of computing the complex mapping $\Phi_v(\omega)$ and $\Phi_e(\omega)$, the inverse mapping Φ_v^{-1} and Φ_e^{-1} (or $\Omega(v_i)$ and $\Omega(e_{ij})$) are generated.

In the preprocessing phase, the roadmap G is built without any obstacles in the predefined or local W space (W_l space in the following context). Note that only collision of inner robot is detected for each v_i and e_{ij} in this period. After that, focus goes to mappings $\Omega(v_i)$ and $\Omega(e_{ij})$.

Take computing $\Omega(v_i)$ for example, the robot in the W_l space is first set to the configuration v_i in C space, and then the surfaces of the robot model in that configuration will be sampled with small vertices to locate the voxels obstructed by these surfaces. Compared with the traditional expansive seed method (a seed cell is put inside the robot and expanded in each direction until all cells $\Omega(v_i)$ occupied by the robot are found by collision checker), this strategy avoids explicit collision detection, lowers the amount of data of a specific mapping and makes the mapping of a relatively large G possible. Fig.3 illustrates the idea of surface sampling.

The upper image in Fig.3 shows the results of surface sampling on two manipulators. The mapping results at a certain configuration v_k , namely $\Omega(v_k)$, is shown in the right image of Fig.3. Here voxels occupied by manipulators and obstacles are rendered with red and green cubes respectively. The reason why mappings of a robot could be substituted by the mappings of the robot surface lies in that when collision happens there is sure to be overlapped surface mappings before the overlapping of inner mappings. Thus it is unnecessary to map those space-consuming inner voxels. By employing this strategy, a lot of time and space can be saved that make the mapping of a larger G pragmatic.

After the generation of these samples, voxels occupied by model surfaces can be easily indexed by the coordinates

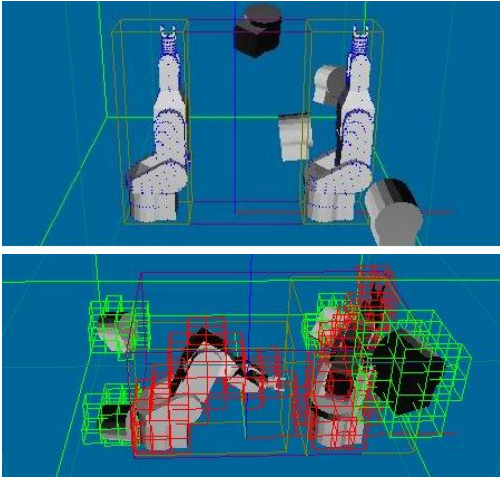


Fig. 3. Surface samples and surface mapping.

of them and the relations between W space and C space could be easily generated. Then these relations are stored as mappings for future usage.

V. OVERVIEW OF THE ALGORITHM

The overview of the anytime planner is shown in Fig.4. The two dash boxes in Fig.4 indicate the roles of subgoal generator and inner replanner respectively.

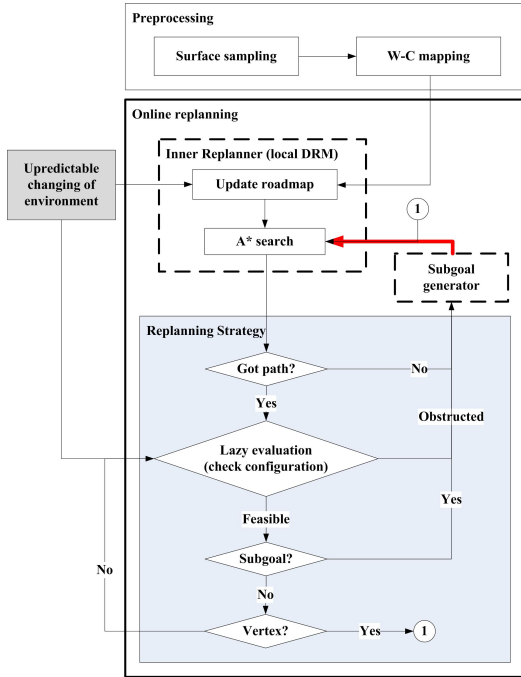


Fig. 4. Overview flowchart of the algorithm

In the beginning, a mapping between ω and G is generated in the preprocessing phase. The W - C mapping box shown in Fig.4 demonstrates this idea. Then these mappings are employed by local DRM to search new paths online. As illustrated previously, when operation of a robot starts, the subgoal generator firstly generates a global path list

$L_{globalpath}$. The first two configurations of $L_{globalpath}$ will then be sent to local DRM as C_{init}^{local} and C_{goal}^{local} to plan a collision free local path.

A. W_l Space and δ_q

One problem during this procedure is how to choose the size of W_l space and the length of step δ_q . Generally speaking, a smaller W_l space implies a faster local DRM. But this is not always the case for the overall planning strategy. If W_l space is too small, the planner may go into local minima easily and have to refer frequently to global planner for help. Also in general cases a larger δ_q could save the cost of a global planner significantly. However, if the step is too large, local mapping may become infeasible.

In reality, a robot should not move out of the current local region with a single step as show in formula (4). Or else it is possible that a subgoal cannot be inserted into the prebuilt roadmap of local DRM and the planner fails to generate a feasible local path.

$$d(q_{new}, base) \leq \text{sizeof}(W_l \text{ space}) \quad (4)$$

In formula (4), $d()$ means the distance between the given configurations and q_{new} denotes the configurations in a RRT. Finally, those q_{new} along the feasible path will serve as subgoals.

$$\min(t(\delta_q, W_l)) \quad (5)$$

$$s.t. \quad \delta_q = f_q(p_{env}) \quad (6)$$

$$W_l = f_w(p_{env}) \quad (7)$$

In fact, how to choose q_{new} and W_l is highly relevant to parameters of the environments p_{env} by function f_q and f_w respectively (constraints (6) and (7)). However, p_{env} cannot be perceived accurately. In the worst case it is even unpredictable. In realization, δ_q and W_l are chosen empirically through lots of experiments in specific scenarios.

B. Adaptive RRT and Replanning

Another problem is when to replan (this is also related to the dynamicity of subgoals). The blue area in Fig.4 demonstrates the replanning strategy employed in our realization.

A key point in this course is the adaptive tuning of P_b . In the beginning P_b is set to 1. When planning fails, our planner will increase P_b by a certain amount to make a more randomized expanding direction. When a new planning (this happens at subgoals) is required, P_b is set back to 1 and readapts itself. This helps a lot in saving energy (or making the results smooth) and getting out of local minima. In fact, thanks to the employment of adaptive P_b tuning, our planner is as probability complete as raw RRT.

As shown in the blue area of Fig.4. The planner replans each time it encounters a perspective collision in the next step. In the following part we will demonstrate the idea lies behind the scheme.

Generally speaking, whether to replan for a new path depends on the requirements of safety or the distance between

obstacles and robots. Based on the idea of W_l space division, the distance between obstacles and robots can be alternatively evaluated by potential fields. Fig.5 illustrates this idea. In Fig.5 the cube indicates the robot while the cuboid indicates the obstacles. Immediate ω_s of them are denoted with stroked grids respectively. The white segments show the generated global path and the red segments show the local details. The bounding box is W_l space. When the obstacles in W_l space is perceived, the planner will compute the potential fields based on the ω_s in W_l space. At a specific configuration v_i , the alternative evaluation will be the largest potential at all $\Omega(v_i)$, refer to (8).

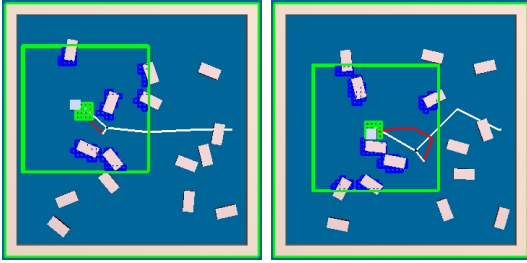


Fig. 5. Distance evaluation using potential fields

$$s(R) = \max(p(\Omega(v_i))) \quad (8)$$

In formula (8), R denotes the robot, $s()$ denotes the evaluation and $p()$ denotes the potential. Since this W_l space potential field approach is carried out in a limited workspace, computational complexity is fine enough for real-time application.

$$s(R) \leq 1 \leftrightarrow 0\text{-hard problem} \leftrightarrow \text{exact CD} \quad (9)$$

In another view, $s(R)$ is like the θ -hard [21]. In the hardest situation (0-hard problem), the calculation of $s(R)$ degenerates into an exact collision detection (CD), refer to formula (9).

Now the approach becomes seeking a minimum $t(\delta_q, W_l, s(R))$. Note that δ_q and W_l are independent of $s(R)$ and they are chosen according to the strategy illustrated in the previous section. Here the discussion will focus on $s(R)$.

In order to ensure completeness, our approach takes planning problems as 0-hard ones and carries out replanning when $s(R) \leq 1$. This schema is implemented as following. $s(R)$ is not calculated explicitly while the potential evaluation approach is substituted with the combined exact collision detection and rough voxel testing to ensure a successful planner in the most rigid environments. The blue area in Fig.4 (the planner replans each time it encounters a perspective collision in the next step) demonstrates the specific steps of this idea.

VI. EXPERIMENTS

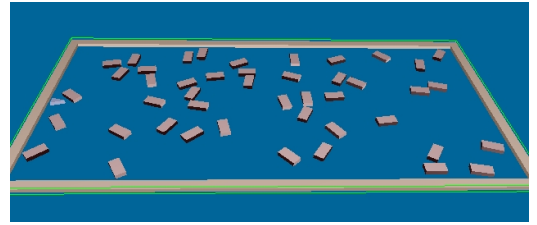
In order to evaluate the proposed method, hundreds of simulation experiments are implemented in 3D workspace with different scenarios. The experimental design mainly

focuses on the ability to plan in the presence of large scenarios and unpredictable changing obstacles.

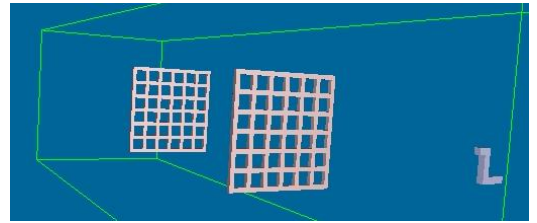
We ascribe these experiments into three groups where each group of experiments includes randomly moving obstacles and a different scale of scenario. Our experimental obstacles move and rotate by a random step along with time. Since the step is random, the obstacles become unpredictable.

All our experiments are carried out on an ordinary personal computer with Pentium D 2.80GHz CPU and 2GB memory. Dynamics in these experiments is implemented with the Open Dynamic Engine. Experimental results are based on an average of 100 executions.

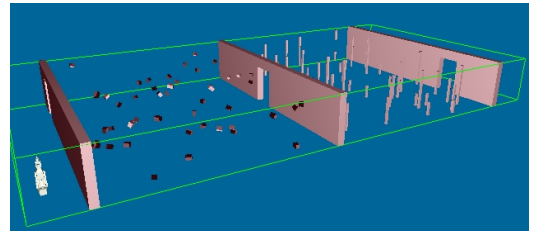
Fig.6 demonstrates the scenarios of our environments.



(a) Scenario of experiment group I



(b) Scenario of experiment group II



(c) Scenario of experiment group III

Fig. 6. The scenario of experiment group I, II and III

The first group of experiments is to plan a 3 DOF vehicle among other unpredictable obstacles. All these objects are supposed to move on the ground (they cannot fly). In the second group of experiments, a 6 DOF space robot is planned to go through randomly rotating latticed obstacle. This scenario forms 'narrow passages' in dynamic environments. In the last group the algorithm is tested against a more complicated environment with stationary/randomly changing obstacles and a 9 DOF mobile manipulator. The manipulator in experiment group III is modeled by parameters of a practical 6 DOF Kawasaki manipulator (FS03N). The original manipulator is mounted on a vehicle base for mobility.

Settings of these experimental environments are listed in Table I.

Here, r , o_i , s and n_o in Table I represent robot size, the

TABLE I
DIFFERENT SCENARIOS OF THE EXPERIMENTS

Sizes	Group I	Group II	Group III
r	$7 \times 6 \times 2$	$5 \times 5 \times 1$	$160 \times 244 \times 136$
o_0	$5 \times 10 \times 2$	$10 \times 15 \times 10$	$10 \times 15 \times 10$
o_1	—	—	$6 \times 6 \times 40$
o_2	—	—	$6 \times 6 \times 80$
o_3	—	—	$6 \times 6 \times 120$
o_4	—	—	$720 \times 20 \times 140$
s	$240 \times 120 \times 2$	$50 \times 50 \times 200$	$720 \times 1440 \times 136$
n_o	45	2	45, 15, 15, 15, 3

size of the i_{th} obstacle, scene size and number of obstacles respectively. The sizes shown in Table I are the AABB bounding box of the objects. For example, the robot in group I is a triangle cuboid, but only the AABB bounding box $7 \times 6 \times 2$ is given here to describe the shape roughly. Note that this is only for the convenience of showing the dimensions, collision detection itself is tested at each mesh exactly.

The motions of the unpredictable obstacles are defined according to reality. They are depicted by six parameters indicating the random walk steps along and rotation steps around the three Cartesian coordinates. The random walk steps are randomly chosen in $(-5, 5)$ while the random rotation steps are chosen in $(-60, 60)$. Note that the lattice obstacles in Group II are special. They rotate with a random step in $(-30, 30)$.

TABLE II
THE SETTINGS OF RANDOMIZED DRM

Settings	Group I	Group II	Group III
δ_q	30, 120	15, 60	120, 120
l_{size}	60×60	$25 \times 25 \times 25$	$240 \times 240 \times 136$
l_{verts}	100	5000	3000
$l_{mapping}$	0.44MB	63.72MB	23.51MB
δ_q	20, 90	15, 60	120, 120

TABLE III
EXPERIMENTAL RESULTS (IN SECONDS)

-	Group I	Group II	Group III
l_{avr}	0.007	0.101	0.144
l_{min}	0.002	0.006	0.014
l_{max}	0.011	0.233	0.299
g_{avr}	0.0	0.0	0.039
g_{min}	0.0	0.0	0.003
g_{max}	0.0	0.0	0.071
t	0.007	0.101	0.184
c_{replan}	47.36	19.96	62.50

Table III shows the result of our approach by comparing the three groups together. In a low dimensional or moderately crowded environment (*Group I* and *Group II*), the global planner in our approach can rapidly generate a high-level guide path ($g_t < 0.001s$ and shown as 0.0 in Table III). Even in a high dimensional and drastically crowded environment (*Group III*), the global planner in our approach is able to return a path in less than 0.1s.

As explicated previously, the computational complexity of our local planner mainly depends on the A* search

algorithm. Since the roadmap in *Group II* and *Group III* is complicated (5000 and 3000 vertices respectively as shown in Table II), the A* takes more time and results in an average local planning cost of 0.101s and 0.144s. The local planner takes little time (0.007s) on the 100-vertex roadmap of *Group I*.

Time cost of the planner in *Group III* becomes higher than 0.15s. This is mainly caused by three factors. The first one is that each new sampled point of the global planner has to do an extra test of self collision. The second factor is the crowded obstacles, and the third one is the large dimension of these scenarios. Although the environment is unpredictable and relatively large, the planner is still sufficient to be employed in real-time (about 0.18s per planning).

The last row c_{replan} in Table III denotes the average times of replanning invoked during each execution (the whole procedure that a robot moves from initial configuration to goal configuration). c_{replan} reflects the robustness of our planner. For instance, even if a planner is fast enough for anytime replanning, it may still fail due to redundant replannings or traps of local minima. In the worst case, c_{replan} goes infinite that the robot cannot find any of the feasible paths. In our experiments, the randomize DRM planner could return the paths in limited replanning times (average 62.50s in the worst case) indicating its completeness.

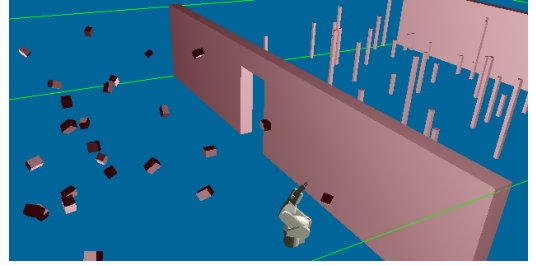


Fig. 7. A detail view of Group III

Table IV shows results of different parameters applied to third experimental group (Fig.7 shows a detail view). In the worst cases, the planner degenerates into a raw RRT planner (first row) or degenerates into a raw DRM planner (last row). Parameter selection seeks the balance between the step length and local size. Note that c_{replan} is shown by c_{min} , c_{max} and c_{avr} in detail.

We also carried out experiments to compare our approach with a collaborative RRT-RRT planner that employs global-RRT as the subgoal generator while employs localRRT as the inner planner for comparison. See Table V.

Although local RRT strategy reduces c_{replan} , RRT-RRT is not a competent planner. In the worst case of a local RRT, the planner takes more than 2.0s to generate a feasible path and it is not qualified for anytime invoking.

In these experiments we can see that even in the most complicated scenario, the cost of a global planner is still less than 0.10 seconds. At the same time, the cost of a local planner does not increase much owing to the prebuilt mappings of DRM. The experimental results confirm our

TABLE IV
EXPERIMENTAL RESULTS OF *Group III* (DIFFERENT PARAMETERS)

Planning Task	δ_q	l_{size}	l_{verts}	l_{min}	l_{max}	g_{min}	g_{max}	t_{avr}	c_{min}	c_{max}	c_{avr}
Task.1-100	5, 30	—	—	—	—	—	—	$\gg 2.0$	—	—	$\gg 1000$
Task.101-200	60, 60	$120 \times 120 \times 136$	2000	0.009	0.227	0.007	0.031	0.169	332	565	429.17
Task.201-300	60, 60	$120 \times 120 \times 136$	3000	0.012	0.233	0.003	0.027	0.167	125	223	155.62
Task.301-400	60, 60	$120 \times 120 \times 136$	5000	0.010	0.253	0.008	0.033	0.227	74	99	86.37
Task.401-500	120, 120	$240 \times 240 \times 136$	3000	0.010	0.205	0.0	0.035	0.184	55	82	62.50
Task.501-600	120, 120	$240 \times 240 \times 136$	5000	0.024	0.344	0.004	0.024	0.258	56	77	60.01
Task.601-700	360, 240	$720 \times 720 \times 136$	5000	0.017	0.301	0.003	0.029	0.272	—	—	$\gg 1000$
Task.701-800	—	$720 \times 1440 \times 136$	—	—	—	—	—	—	—	—	—

TABLE V
EXPERIMENTAL RESULTS ON *Group II* AND *III* (RRT-RRT)

<i>Group II</i>	Settings	t_{avr}	c_{replan}
globalRRT	Step : 15, 60	0.0	11.73
localRRT	Step : 1, 10	1.077 (0.0, 2.741)	—
Total	—	1.077	—
<i>Group III</i>	Settings	t_{avr}	c_{replan}
globalRRT	Step : 120, 120	0.032	23.75
localRRT	Step : 5, 30	$\gg 2.0$ (0.0, $\gg 2.0$)	—
Total	—	$\gg 2.0$	—

assumption that the collaboration of subgoal generator and inner replanner is mighty. The subgoal based planner can be employed in relatively large scenarios with unpredictable obstacles at anytime.

VII. CONCLUSIONS

In this paper a novel path planning algorithm is proposed aiming at generating a collision free path for mobile agents in unpredictable environments. The planner is composed of a subgoal generator and an inner replanner based on the idea of RRT and DRM respectively. Potential field based collaboration between the multiple shot and single shot primitives from RRT and DRM helps to generate subgoals dynamically and plan paths rapidly. Experimental results and analysis show that our method can not only perform path planning rapidly while avoiding unpredictable obstacles but also be competent for relatively large scenario scales.

ACKNOWLEDGEMENTS

This work is supported by National Natural Science Foundation of China (NSFC, No.60875050, 60675025), National High Technology Research and Development Program of China (863 Program, No.2006AA04Z247), Shenzhen Scientific and Technological Plan and Basic Research program (No.JC200903160369A), Natural Science Foundation of Guangdong(No.9151806001000025).

REFERENCES

[1] L. E. Kavraki, P. Svestka, J. C. Latombe and M. H. Overmars, "Probabilistic roadmaps for fast path planning in high-dimensional configuration spaces", in *IEEE Transactions on Robotics and Automation*, pp. 566-580, 1996.

[2] S. M. LaValle and J. J. Kuffner, "Rapidly-exploring random trees: Progress and prospects", in *Workshop on Algorithmic Foundation of Robotics*, 2000.

[3] D. Hsu, R. Kindel, J. C. Latombe and S. Rock, "Randomized kinodynamic motion planning with moving obstacles", in *International Journal of Robotics Research*, pp. 233-255, 2002.

[4] L. Jaillet and T. Simeon, "A PRM-based motion planner for dynamically changing environments", in *IEEE/RSJ International Conference on Intelligent Robots and Systems*, pp. 1606-1611, 2004.

[5] J. P. van den Berg, Promotor: M. H. Overmars, "Path Planning in Dynamic Environments", Ph. D. Thesis, 2007.

[6] J. Vannoy and J. Xiao, "Real-time Adaptive Motion Planning (RAMP) of Mobile Manipulators in Dynamic Environments with Unforeseen Changes", in *IEEE Transactions on Robotics*, pp. 1199-1212, Oct. 2008.

[7] S. M. LaValle, "Planning algorithms", Cambridge University Press, 2006.

[8] D. Hsu, J. C. Latombe and R. Motwani, "Path Planning in Expansive Configuration Spaces", in *International Journal of Computational Geometry and Applications*, pp. 495-512, 1999.

[9] C. Nielsen and L. Kavraki, "A two level fuzzy PRM for manipulation planning", in *IEEE/RSJ International Conference on Intelligent Robots and Systems*, pp. 1716-1721, 2000.

[10] R. Bohlin and L. E. Kavraki, "Path planning using Lazy PRM", in *IEEE International Conference on Robotics and Automation*, pp. 521-528, 2000.

[11] P. Leven and S. Hutchinson, "Toward real-time path planning in changing environments", in *Workshop on the Algorithmic Foundations of Robotics*, pp. 363-376, 2000.

[12] M. Kalmann and M. Mataric, "Motion planning using dynamic roadmaps", in *IEEE Transactions on Robotics and Automation*, pp. 4399-4404, 2004.

[13] H. Liu, X. Z. Deng and H. B. Zha, "A path planner in changing environments by using W-C nodes mapping coupled with lazy edges evaluation", in *IEEE/RSJ International Conference on Intelligent Robots and Systems*, pp. 4078-4083, 2006.

[14] E. Plaku, K. E. Bekris, B. Y. Chen, A. M. Ladd and L. E. Kavraki, "Sampling-based roadmap of trees for parallel motion planning", in *IEEE Transactions on Robotics*, pp. 587-608, 2005.

[15] P. C. Chen and Y. K. Hwang, "SANDROS: A dynamic graph search algorithm for motion planning", in *IEEE Transactions on Robotics and Automation*, pp. 390-403, 1998.

[16] S. Candido, Y. T. Kim and S. Hutchinson, "An improved hierarchical motion planner for humanoid robots", in *IEEE-RAS International Conference on Humanoid Robots*, pp. 654-661, 2008.

[17] J. J. Kuffner and S. M. LaVelle, "RRT-Connect: An efficient approach to single-query path planning", in *IEEE International Conference on Robotics and Automation*, pp. 995-1001, 2000.

[18] J. Bruce and M. Veloso, "Real-time randomized path planning for robot navigation", in *IEEE International Conference on Intelligent Robots and Systems*, pp. 2383-2388, 2002.

[19] D. Ferguson, N. Kalra and A. Stenz, "Replanning with RRTs", in *IEEE International Conference on Robotics and Automation*, pp. 1243-1248, 2006.

[20] M. Zucker, J. J. Kuffner and M. Branicky, "Multipartite RRTs for rapid replanning in dynamic environments", in *IEEE International Conference on Robotics and Automation*, pp. 1603-1609, 2007.

[21] O. Brock and L. E. Kavraki, "Decomposition-based Motion Planning: A Framework for Real-time Motion Planning in High-dimensional Configuration Spaces", in *IEEE International Conference on Robotics and Automation*, pp. 1469-1474, 2001.